Composite Structures 182 (2017) 209–222

Contents lists available at ScienceDirect

Composite Structures

journal homepage: www.elsevier.com/locate/compstruct

Large deformation of an arc-Miura structure under quasi-static load

X.M. Xiang[a,b], G. Lu[a,*], D. Ruan[a], Z. You[c], M. Zolghadr[a]

[a] Faculty of Science, Engineering and Technology, Swinburne University of Technology, Hawthorn, Vic 3122, Australia
[b] Tianjin Key Laboratory of Civil Structure Protection and Reinforcement, Tianjin Chengjian University, Tianjin 300384, China
[c] Department of Engineering Science, University of Oxford, Parks Road, Oxford OX1 3PJ, UK

ARTICLE INFO

Keywords:
Arc-Miura
Monolithic arch
Quasi-static compression
Parametric study

ABSTRACT

Miura-Ori based foldcores have been regarded as a potential substitute for conventional honeycomb cores due to many advantages, such as open structure and continuous manufacturing process. Arc-Miura foldcore is one of the Miura-derivative cores which does not have curvature limitations. In this research, the arc-Miura specimens were successfully manufactured using a stamping process and tested under a quasi-static out-of-plane compressive load. An explicit finite element analysis (FEA) of arc-Miura models was developed and validated with the experimental results. Furthermore, a parametric study of arc-Miura models subjected to quasi-static out-of-plane compression was performed, through which the relationships between the mechanical properties and the geometric parameters were established. Finally, the mechanical properties of arc-Miura models and corresponding monolithic arches were compared. It was shown that arc-Miura patterns perform better than the corresponding monolithic arches in terms of force and energy absorption.

1. Introduction

Origami foldcores were proposed during the late 1990's which are basically constructed by folding a sheet using an origami pattern. Origami-inspired structures offer many advantages such as foldability and deployability. These features enable the structure to be compactly stowed in a relatively small package and have good structural performance in the deployed form. For military applications, origami-inspired deployable shelters offer important advantages as they require a very small space in a folded form during transportation [1,2].

One of the most common patterns to make origami foldcores is known as Miura pattern, in which the foldcore is fabricated by folding the sheet along a pattern with straight and zigzag creases [3]. Miura-based origami foldcores possess many useful characteristics, such as rigid foldability, and therefore they have been used in engineering, architectural and design applications. Deformation of Miura pattern foldcores is completely realized by the folding/ unfolding at the creases and does not involve any deformation of the rigid faces [4]. Due to this characteristic, Miura-based origami foldcores can be manufactured easily from sheet materials such as plastics, papers, metals or composites [5,6]. Parametrisations have been established to investigate the relationships between crease pattern, volumetric, and kinematic parameters [7–9].

Mechanical properties of origami patterns have been widely investigated. Honeycomb core has better performance in compression, while flat Miura-based folded cores have comparable or even better performance in the shear and bending cases [10]. Experimental and numerical studies of curved-crease and indented foldcores under quasi-static out-of-plane loads have been conducted by Gattas and You [11,12]. They found that these modified foldcores have significantly higher energy-absorption capability than straight-crease foldcores. Kirigami-inspired folded core structures were also investigated by means of experiment and numerical simulation by the same research group [13]. The diamond cube strip core offered a much higher increase in average force compared with the best-performing curved-crease and the standard Miura-type foldcore [13].

Out-of-plane compression, three-point bending and in-plane compression tests on Elvaloy Miura-ori patterned sheet were carried out by Liu et al. [14]. Based on their simulation results, the deformation patterns and the energy absorption capacity were investigated. Experimental and numerical studies on thermoplastic foldcore (PET and PEEK foldcore) were studied and the result showed that thermoplastic foldcore had comparable or even better energy absorption performances than the aramid one [15].

Research was conducted by numerical simulation and experiment on the axial crushing performance of thin-walled tubes with origami patterns in terms of initial peak force and energy absorption [16,17]. Other origami structures, e.g., the unit cell with two zigzag strips surrounding a hole with a parallelogram shape [18] and cylindrical foldcore [19], have also been investigated using FEA method. Theoretical

* Corresponding author.
E-mail address: glu@swin.edu.au (G. Lu).

http://dx.doi.org/10.1016/j.compstruct.2017.09.023
Received 12 May 2017; Received in revised form 22 August 2017; Accepted 14 September 2017
Available online 18 September 2017

analysis of the structural mechanics of folded origami were also analyzed associated with the expansion kinematics of the foldcores [20,21]. Mechanical properties of both periodic and non-periodic origami patterns were studied theoretically by Lv et al. [22], and they found both negative and positive Poisson's ratios of Miura-ori structures. Origami structures were investigated as the core of sandwich structures, and they were found to improve shell bending stiffness and higher strength/weight ratios [23,24].

Although many aspects of the mechanical behaviours of flat origami-based foldcores have been studied widely in recent years, very limited studies have been conducted on curved Miura-ori structures, which could be used as the foldcores of curved sandwich panels. In this paper, large deformation of arc-Miura structure has been investigated. Two boundary conditions are considered: free ends and clamped ends. Quasi-static out-of-plane compression experiments are conducted first, followed by detailed finite element analyses. A parametric study is conducted to observe the influences of geometric parameters on mechanical performance.

2. Geometry of arc-Miura pattern

2.1. Parameters of the arc-Miura pattern

The Miura pattern is achieved by repeating a unit cell geometry along two axes on the same plane. The unit cell geometry consists of four identical parallelograms defined by three parameters, a, b and ϕ (Fig. 1). Miura foldcore is produced by folding a sheet with the Miura pattern along its straight and zigzag creases. The solid and dashed lines denote the mountain and valley creases respectively. The arc-Miura pattern is one of the first-level derivatives of Miura patterns, which possesses the characteristics of developability, flat-foldability, rigid-foldability and tessellation similar to the Miura pattern. The term "first level derivative" signifies that the geometry is obtained by modifying only one characteristic of the Miura pattern, i.e. crease alignment. Fig. 2 illustrates the arc-Miura pattern derived from the Miura pattern by altering the alignment of zigzag creases. The red dashed line is the altered zigzag crease in comparison with Fig. 1. The solid and dashed lines also denote the mountain and valley creases respectively.

The zigzag creases in Fig. 2 alter the geometry of the arc-Miura from the Miura pattern. Fig. 3 demonstrates the folding stages of the arc-Miura pattern. A cylindrical coordinate system was built shown in Fig. 3(c). Coordinates r and θ define the radius and the fold angle of the arc-Miura, and coordinate z is in the width direction. The arc-Miura unit cell is formed from four identical trapezoids (Fig. 2(b)). This alteration in the Miura pattern introduces a set of different parameters a_1, a_2, b_1, b_2, ϕ_1 and ϕ_2, with the requirement that $a_1 < a_2$, $b_1 < b_2$ and $\phi_2 < \phi_1 < 90°$. Unlike the flat Miura pattern, the crease pattern parameters in the arc-Miura unit cell are not independent of each other. Eqs. (1) and (2) can be obtained by considering an arc-Miura unit cell trapezoid (see Fig. 2(b)).

$$b_1\sin\phi_1 = b_2\sin\phi_2 \tag{1}$$

$$b_1\cos\phi_1 + a_2 = b_2\cos\phi_2 + a_1 \tag{2}$$

Gattas et al. [25] presented a parametric model to define the geometry of the arc-Miura pattern. Fig. 4 illustrates the configuration variables and $(r-\theta)$ projection of an arc-Miura pattern with similar variable names defined by them [25]. θ_A, θ_{VZ} and θ_{MZ} are the dihedral angles, while η_{VA}, η_{VZ}, η_{MA} and are the edge angles (see Fig. 4(a)). Furthermore, Eqs. (1) to (12) express the relation between all parameters of the arc-Miura parametric model introduced in Ref. [25].

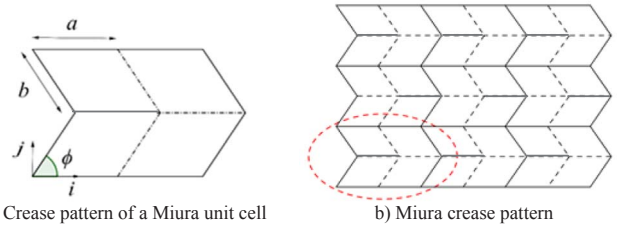

a) Crease pattern of a Miura unit cell b) Miura crease pattern

Fig. 1. Flat Miura pattern.

$$(1+\cos\eta_{MZ})(1-\cos\eta_{MA}) = 4\cos^2(\phi_1) \tag{3}$$

$$(1+\cos\eta_{VZ})(1-\cos\eta_{VA}) = 4\cos^2(\phi_2) \tag{4}$$

$$\cos\eta_{MA} = \sin^2\phi_1\cos\theta_{MZ} - \cos^2\phi_1 \tag{5}$$

$$\cos\eta_{VA} = \sin^2\phi_2\cos\theta_{VZ} - \cos^2\phi_2 \tag{6}$$

$$\cos\eta_{MZ} = \sin^2\phi_1\cos\theta_A + \cos^2\phi_1 \tag{7}$$

$$\cos\eta_{VZ} = \sin^2\phi_2\cos\theta_A + \cos^2\phi_2 \tag{8}$$

$$\xi = \eta_{VA} - \eta_{MA} \tag{9}$$

$$R_i^2 = \frac{a_1^2 + a_2^2 - 2a_1a_2\cos\eta_{MA}}{2(1-\cos\xi)} \tag{10}$$

$$R_o^2 = \frac{a_1^2 + a_2^2 - 2a_1a_2\cos\eta_{VA}}{2(1-\cos\xi)} \tag{11}$$

$$w_u = 2b_1\sin(\eta_{MZ}/2) = 2b_2\sin(\eta_{VZ}/2) \tag{12}$$

Eqs. (1) to (12) are sufficient to determine the folded geometry of an arc-Miura pattern regardless of which five geometrical parameters are chosen as the inputs. In this research, an inverse design method has been used to re-formulate Eqs. (1) to (12) in order to facilitate calculation of the unit cell geometrical parameters of the arc-Miura pattern with constrained volumetric parameters, i.e. the inner radius (R_i), outer radius (R_0), fold angle (ζ) and unit cell width (w_u). Five inputs are required in order to calculate the other twelve parameters. In this study, these five parameters were chosen to be the four aforementioned volumetric parameters (R_i, R_0, ζ and w_u), as well as one crease pattern parameter i.e. a_1. It should be noted that due to the geometrical constraints, a_1 cannot be assigned any random number unless the number is between two extreme values. These extreme values for a_1 are determined by the volumetric parameters, R_i, R_o, and ζ. Fig. 5 illustrates the extreme positions for both a_1 and a_2. The position of the joint where the a_1 and a_2 lines cross each other on the outer curve must remain between points B and C. Eqs. (13) and (14) define the conditions for a_1 anda_2 implied in Fig. 5.

$$R_o - R_i < a_1 < \sqrt{R_i^2 + R_o^2 - 2R_iR_o\cos(\xi/2)} \tag{13}$$

$$\sqrt{R_i^2 + R_o^2 - 2R_iR_o\cos(\xi/2)} < a_2 < \sqrt{R_i^2 + R_o^2 - 2R_iR_o\cos\xi} \tag{14}$$

The parametric model was developed using SolidWorks software. The parameters R_i, R_0, ζ, W_u and a_i were defined as the inputs, and the other parameters were calculated by the software, then the 3D model of a unit cell was developed. Two other parameters required were the number of units in the tangential direction (m), and the number of cells in the lateral direction (n). This developed a structure consisting of $m \times n$ cells.

2.2. Nominal density

The front view of the arc-Miura structure is shown in Fig. 6. The area of flat surface in each unit (see Fig. 2(a)) is

$$S = 2(a_1 + a_2)b_2\sin\varphi_2 \tag{15}$$

The volume occupied by each unit (see Fig. 6) is

$$V = \pi(R_o^2 - R_i^2)\cdot\frac{\xi}{2\pi}\cdot w_u = \frac{\xi}{2}(R_o^2 - R_i^2)w_u \tag{16}$$